

# Prestressed FRP Flexural Strengthening of Softwood Glue - Laminated Timber Beams

**James F. Brady**  
**Ph.D. Candidate**

**Department of Civil Engineering, National University of Ireland, Galway (NUIG)**  
**Galway, Ireland**

**Annette M. Harte**  
**Senior Lecturer**

**Department of Civil Engineering, National University of Ireland, Galway (NUIG)**  
**Galway, Ireland**

## Summary

Brittle failure of glue-laminated (glulam) timber beams usually occurs on their tension faces. Fibre-reinforced plastic (FRP) composite laminates, bonded to the beam soffit, have successfully been used to enhance their structural performance and induce ductile/plastic compression behaviour. The bending strength, stiffness and ductility can be further improved by pre-tensioning the FRP before bonding it in the tension zone of the glulam beam.

Analytical models to predict the stiffness and flexural strength of prestressed FRP reinforced glulams are outlined in this paper. The elastic-plastic behaviour of FRP reinforced timber and various failure modes are incorporated. The theoretical results indicate that the performance of low-strength timber can be significantly enhanced by prestressing with FRP composites.

## 1. Introduction

Glue-laminating is a well-established technique for minimising the effect of strength reducing defects that exist in low-grade solid timber beams. Improvements in structural performance have been achieved by bonding fibre-reinforced plastic (FRP) composite laminates, which have a high strength-to-weight ratio, to the tension face of the glulam beam [1]. Failure of an unreinforced glulam normally occurs in the bottom laminate and is usually initiated by the presence of a knot. FRP reinforcement changes the mode of failure from that of brittle tension nature to a more predictable ductile/plastic compressive mode.

The primary objective of the research described in this paper is to examine the feasibility of further increasing the flexural strength, stiffness and ductility of low strength, home-grown Sitka spruce glulam beams by bonding pre-tensioned FRP laminates in the tension zone. By applying a prestress, the FRP material may be more efficiently used, since a greater portion of its tensile strength is engaged. As a result, the quantity of fibres required and costs are reduced. Prestressing effectively increases flexural strength by introducing an initial compressive stress into the timber fibres that in service are under tension. The application of prestress via an eccentric tendon causes the beam to bend upwards along its length. This pre-camber will offset deflection under loading and effectively increase stiffness.

Initial efforts at prestressing timber considered readily available steel as reinforcement [2]. The ratio of the ultimate strain of FRP to that of steel is approximately 2.5 - 3.5 to 1. This means that FRP will stretch more than steel if both are prestressed to the same percentage of their ultimate tension strength (UTS). Therefore, prestress loss, due to elastic shortening and creep of the timber, when using FRP will be less than that associated with steel.

Limited research on timber beams reinforced with bonded prestressed FRP laminates has been reported. Analytical and experimental studies on the flexural behaviour of prestressed carbon FRP reinforced defect-free beams demonstrate their superior performance [3]. The benefit of prestressing low strength, inexpensive timber with relatively cheap glass FRP has undergone very little investigation. *Rodd et. al. (2003)* [4] is the only study known to the author that considered prestressed glass FRP reinforcement of low quality UK softwood. An increase in bending strength of 43% was reported.

With the exception of *Rodd et. al. (2003)* [4], all the investigations referred to above, considered timber beams reinforced with a FRP laminate bonded directly onto the tension soffit. In practice, an additional timber laminate, referred to in this paper as a bumper, is often bonded below the FRP to improve fire performance and aesthetics. The effect of this timber facing on load-deflection behaviour of non-prestressed glulams was examined by *Romani et. al. (2001)* [5] who found that the load-carrying capacity dropped sharply after the initial failure of the bumper laminate. However, the load capacity then increased until a subsequent global failure of the glulam above the FRP occurred.

This paper describes analytical models developed to predict the stiffness and ultimate flexural strength of prestressed FRP reinforced glulams containing a bumper laminate. The behaviour of FRP-prestressed glulams in comparison with unreinforced and non-prestressed FRP reinforced beams is examined. The models incorporate the initial failure of the bumper and the global failure of the glulam above the FRP. The plastic compression behaviour of timber and different failure modes, depending on the ratio of tension and compression strength, are taken into account.

## 2. Theoretical Basis of Models

### 2.1 Stiffness Model

The initial location of the neutral axis from the tension face,  $y_{Et,max}$  and the stiffness,  $E_E I_E$  are calculated using a series of transformed section analyses (TSA), according to the theory of a composite section in a linear-elastic state. The TSA is carried out with and without a bumper laminate to take into account the shift in the neutral axis after the bumper fails in a linear-elastic state. The location of the neutral axis,  $y_{Et,max}$  is calculated from Equation 1.

$$y_{Et,max} = \frac{\sum(A_{eq,i} \bar{y}_i)}{\sum A_{eq,i}} \quad (1)$$

where  $A_{eq,i}$  = transformed cross-sectional area of each constituent laminate, i.

$\bar{y}_i$  = distance from the tension face to the centroidal axis of each constituent, i.

The second moment of area,  $I_E$  of a FRP reinforced glulam beam is determined by applying the parallel axis theorem to the transformed cross-section using Equation 2.

$$I_E = \sum(I_i + A_{eq,i} y_{Eg,i}^2) \quad (2)$$

where  $I_i$  = second moment of area of each constituent part, i of the composite beam.

$y_{Eg,i}$  = distance from the neutral axis of the transformed section to the centroidal axis of each constituent part, i (i.e.)  $|y_{Et,max} - \bar{y}_i|$ .

The stiffness,  $E_E I_E$  of the composite glulam is then calculated by multiplying  $I_E$  by the modulus of elasticity (MOE) of the laminate to which all the constituent parts were transformed.

### 2.2 Flexural Strength Model

The flexural strength model estimates the moment capacity ( $M_u$ ), modulus of rupture ( $MOR$ ), and the ultimate bending strength (UBS /  $f_{mu}$ ) of unreinforced glulams and non-prestressed and prestressed FRP reinforced glulams, based on the uniaxial compression and tension strengths of the timber,  $f_{Tcu}$  and  $f_{Ttu}$ . The variation in strain and stress through the depth of the cross-section and load-deflection curves can be plotted. The model is based on the stress-strain relationship and modes of failure of unreinforced timber proposed by *Buchanan (1990)* [6]. The fact that the tensile stress at failure in bending,  $f_{mu}$  is greater than that at failure in uniaxial tension,  $f_{Ttu}$  is taken into account by calibration with unreinforced bending tests. The tension strength,  $f_{Ttu}$  will effectively be increased with the addition of FRP. The model is modified to account for this effect and calibrated with bending tests on FRP reinforced beams.

## 2.2.1 Timber Stress-Strain Relationship

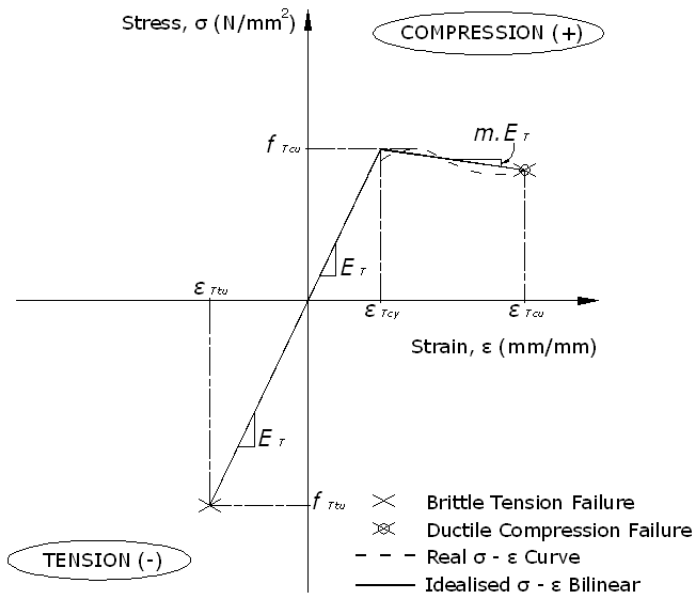


Fig. 1 Idealised bi-linear elastic-plastic uniaxial stress-strain relationship at failure

## 2.2.2 Modes of Failure

The UBS of a FRP reinforced glulam depends on the mode of failure. In general, four distinct failure modes are possible in defect-free wood, depending on the ratio of the ultimate tension and compression strengths [6]. In this paper, these modes are referred to as pure tension, partial tension, partial compression and pure compression failure. For timber that is weaker in tension than in compression, pure tension fracture occurs when the stress in the extreme timber fibres in tension,  $f_{Ttx}$  reaches the UBS,  $f_{mu}$ , while the cross-section is in a linear-elastic stress state. Ductile yielding of the outermost compression fibres begins when the stress in these fibres,  $f_{Tcx}$  reaches the ultimate compression strength,  $f_{Tcu}$  and an elastic-plastic stress distribution develops. Partial tension failure occurs when minimal compression yielding has taken place and occurs in clear wood or FRP reinforced timber which is slightly stronger in tension than in compression. For material that is considerably stronger in tension than in compression, significant compression yielding occurs and the failure is classified as partial compression. For material that is extremely strong in tension compared to compression, pure compression failure occurs if the compressive stress,  $f_{Tcx}$  reaches the UBS,  $f_{mu}$ . This is unlikely to occur in low-grade timber and so is not considered further.

Previous testing indicates that, after failure of the bumper laminate, the load carrying capacity will increase until a subsequent global failure of the glulam above the FRP occurs [5]. Six failure modes of FRP reinforced beams, including a bumper laminate, are incorporated into the model. The six modes are considered in pairs depending on whether or not the bumper laminate is intact.

- (a) & (b) Pure tension fracture of the bumper laminate or the laminate above the FRP.
- (c) & (d) Partial tension fracture of the bumper laminate or the laminate above the FRP.
- (e) & (f) Partial compression failure, with significant compression yielding, of the top laminate, before or after the bumper laminate has failed.

To determine the ultimate moment and UBS, it is necessary to locate the neutral axis for each failure mode. Elementary linear-elastic theory applies to failure modes (a) and (b). In order to locate the position of the neutral axis,  $y_{Et\ max}$  for the elastic-plastic stress distribution, before and after the bumper laminate fails, a quadratic equation was derived that defines its position in terms of the maximum tensile stress induced in bending. Before the model equations are presented, the parameters used to describe the elastic-plastic stress profile are defined. The moment capacity,  $M_u$  is calculated by taking moments of the internal forces about the neutral axis.

The idealised uniaxial stress-strain ( $\sigma - \epsilon$ ) relationship of timber used in the model is shown in Figure 1. Compression behaviour is assumed to be bi-linear elastic-plastic. Once the ultimate compression stress,  $f_{Tcu}$ , with a corresponding yield strain,  $\epsilon_{Tcy}$ , is reached, it is not retained, but decreases linearly, with increasing strains, to a certain ratio,  $r$  of  $f_{Tcu}$ . The slope of the falling branch is a constant ratio,  $m$  of the MOE of the timber,  $E_T$ . In tension, the behaviour is assumed to be linear-elastic to brittle failure.

The FRP is assumed to be linear-elastic to failure with a MOE value,  $E_F$  and ultimate tension strength,  $f_{Fu}$ .

### 2.2.3 Elastic-Plastic Stress Profile Parameters

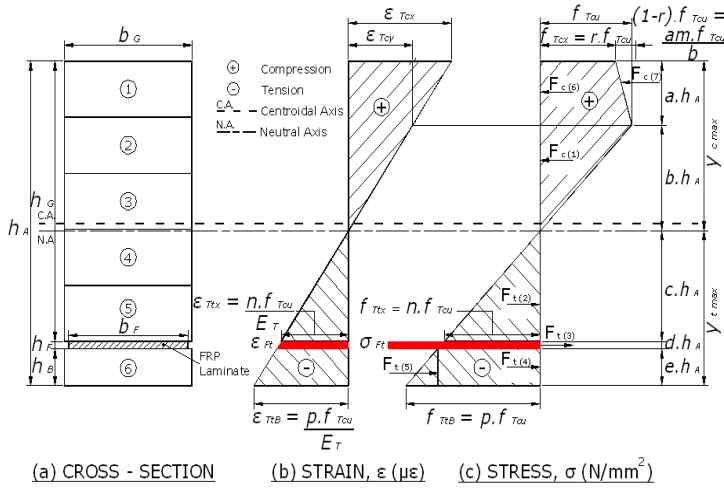


Fig. 2 (a) FRP reinforced glulam cross-section  
(b) & (c) Idealised strain and stress distributions

The idealised strain and stress distributions in a FRP reinforced glulam of total height,  $h_A$  and width,  $b_G$ , when subjected to loading sufficient to cause ductile yielding, are shown in Figure 2. The tension stresses in the laminate above the FRP and the bumper laminate are  $f_{Ttx}$  and  $f_{TtB}$ , respectively, and are expressed as ratios  $n$  and  $p$  of the yield compression stress,  $f_{Tcu}$ . The falling branch of the stress distribution results in a stress in the extreme compression fibres,  $f_{Tcx}$  that is less than the ultimate stress,  $f_{Tcu}$  by a ratio,  $r$ . The FRP stress distribution is simplified to a rectangular block with an average stress,  $\sigma_{Fr}$ . The modular ratio,  $n_T$  is a ratio of the MOE of the FRP to that of the timber.

The parameters  $a$ ,  $b$ ,  $c$ ,  $d$  and  $e$  are ratios of certain heights of the stress distribution relative to the total height of the cross-section,  $h_A$ . The ratio,  $(d + e)$  is expressed as a constant depth ratio,  $A$ .

### 2.2.4 Quadratic Equation to locate the Neutral Axis for Failure Modes (c) and (e)

Using the notation shown in Figure 2(c), the total internal tension and compression forces are:

$$F_t = b_G h_A f_{Tcu} \left[ \frac{p}{2} \left( \frac{c^2}{c+d+e} \right) + n_T p \left( \frac{cd+d^2/2}{c+d+e} \right) + p \left( \frac{ce+de}{c+d+e} \right) + \frac{p}{2} \left( \frac{e^2}{c+d+e} \right) \right] \quad (3)$$

$$F_c = b_G h_A f_{Tcu} \left[ \frac{b}{2} + \left( a - \frac{a}{2}(1-r) \right) \right] \quad (4)$$

For axial force equilibrium, the sum of the total tension and compression forces must be equal to zero. This yields the following quadratic equation used to determine the neutral axis depth ratio,  $c$ .

$$c^2 \left( -p - \frac{1}{p} - 2 - \frac{m}{p} - 2m - mp \right) + c \left( -2n_T pd - 2pe + \frac{2A}{p} + 2 - \frac{4A}{p} - 4A + 2m + 2mp - \frac{2mA}{p} - 4mA - 2mA p \right) - n_T pd^2 - pe(2d+e) - A^2 \left( \frac{1}{p} + 2 \right) + 2A - m \left( p - 2A - 2Ap + \frac{A^2}{p} + 2A^2 + A^2 p \right) = 0 \quad (5)$$

### 2.2.5 Quadratic Equation to locate the Neutral Axis for Failure Modes (d) and (f)

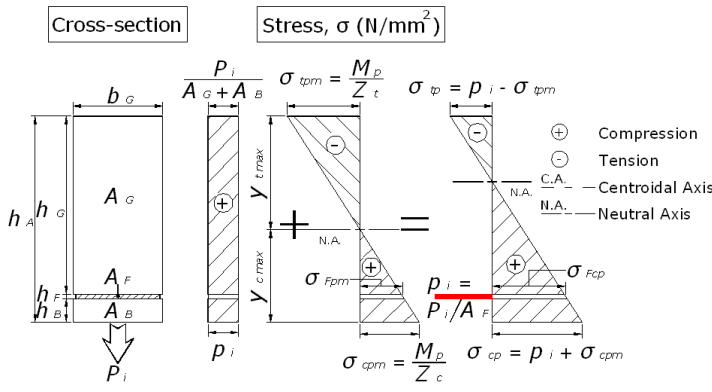
Similarly, a quadratic equation, in terms of the stress ratio,  $n$ , can be obtained to determine the depth ratio,  $c$  after the bumper laminate fails.

$$c^2 \left( -n - \frac{1}{n} - 2 - \frac{m}{n} - 2m - mn \right) + c \left( -2n_T nd + 2 - 2d + 2m(n+1)(1-d) \right) - n_T nd^2 - m(n - 2dn + d^2 n) = 0 \quad (6)$$

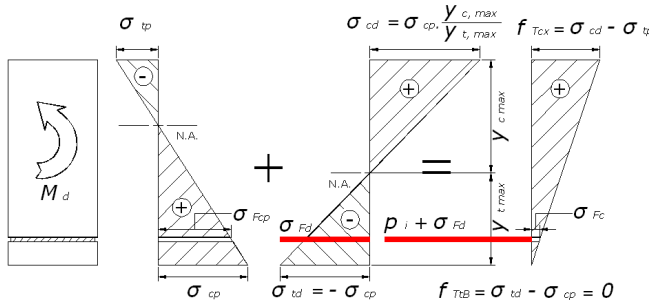
### 2.3 Prestressed FRP Model

In prestressing a glulam, the FRP laminate is stretched and anchored at both ends. The top glulam section and the bumper laminate are then bonded to the FRP. Upon gradual release of the tension load, the prestress is transferred to the timber by the cured adhesive layer. The application of prestress induces compression stress in the bottom of the beam. On the other hand, applied load results in tension stresses in the bottom. As the applied load is increased, the compressive stress in the bottom face of the beam due to prestress gradually reduces to zero. These different stages of flexural response are examined in the strength model using a three-phase analysis [7], as illustrated in Figure 3. The computer model developed for the strength computations determines the stress distribution by incrementally increasing the tension stress in the bottom of the bumper laminate due to the applied loading and finding the corresponding neutral axis position. Therefore, it is essential to determine the applied tension stress required to offset the initial compression stress induced in the bumper due to prestress.

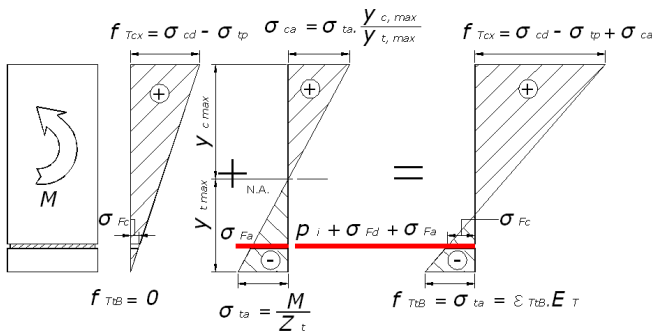
#### 2.3.1 Stage 1 - Prestress Transfer



(a) Stage 1 - Prestress Transfer



(b) Stage 2 - Decompression



(c) Stage 3 - Applied Loading After Decompression

The introduction of a prestressed FRP laminate, located at an eccentricity,  $e$  ( $= y_{t,max} - h_B - h_F/2$ ) below the neutral axis, pre-tensioned to a force,  $P_i$  ( $= p_i \cdot A_F$ ), creates the stress distribution illustrated in Figure 3(a) in the timber, upon prestress release and transfer. The application of this eccentric force in the FRP is equivalent to applying an axial compressive force,  $P_i$  and a hogging moment,  $M_p$  at any given section of the timber. The moment due to the prestress is a product of the pre-tension force and eccentricity (i.e.)  $M_p = P_i \cdot e$ . The axial compressive force component creates a constant axial stress distribution of magnitude,  $p_i$ . The hogging moment causes the beam to deflect upwards or pre-camber along its length, resulting in tension on the top face and compression on the bottom. Therefore, the bending component creates a linear stress distribution with tension and compression stresses,  $\sigma_{tpm}$  &  $\sigma_{cpm}$  at the extreme fibres. It is important to note that the bending stresses induced in the timber due to the prestress are calculated relative to the elastic section moduli of the gross timber cross-section only,  $Z_T$ . On the other hand, the stresses induced in the timber due to applied loading are determined relative to the elastic section moduli of the transformed or equivalent cross-section including the FRP,  $Z_E$ .

The total stresses due to eccentric prestress in the top (tension) fibres,  $\sigma_{tp}$  and the bottom (compression) fibres,  $\sigma_{cp}$  are given in Equations 7 and 8, respectively.

Fig. 3 Three-phase prestress analyses

$$\sigma_{ip} = p_i - \sigma_{ipm} = \frac{P_i}{A_G + A_B} - \frac{M_p}{Z_{Tt}} = p_i - \frac{M_p \cdot y_{Tt, \max}}{I_T} \quad (7)$$

$$\sigma_{cp} = p_i + \sigma_{cpm} = \frac{P_i}{A_G + A_B} + \frac{M_p}{Z_{Tb}} = p_i + \frac{M_p \cdot y_{Tc, \max}}{I_T} \quad (8)$$

where  $Z_{Tt}$ ,  $Z_{Tb}$  = elastic section moduli of timber relative to the top and bottom fibres.

### 2.3.2 Stage 2 - Decompression

In order to reach the load level at which zero stress and strain exists in the bottom of the bumper laminate, an external decompression moment,  $M_d$ , defined by Equation 9, must be applied. The application of  $M_d$  induces the applied decompression tension stress,  $\sigma_{td}$  in the bottom of the bumper laminate and the corresponding compression stress,  $\sigma_{cd}$  in the top of the glulam:

$$\sigma_{td} = \frac{M_d}{Z_{Eb}} = \frac{M_d \cdot y_{Et, \max}}{I_E} = -\sigma_{cp} \quad (9)$$

$$\sigma_{cd} = \sigma_{cp} \cdot \frac{y_{Ec, \max}}{y_{Et, \max}} \quad (10)$$

Combining these incremental decompression stresses with the pre-tension stresses at transfer, the overall stress levels, at the end of the decompression stage, in the bottom and top of the glulam are:

$$f_{TtB} = \sigma_{td} - \sigma_{cp} = 0 \quad (11)$$

$$f_{Tcx} = \sigma_{cd} - \sigma_{ip} \quad (12)$$

The definition of the stress, and corresponding strain, distribution at the end of the decompression phase is an important intermediate step in the prestressing analyses because it enables the distribution at other load levels to be easily established in the flexural strength model.

### 2.3.3 Stage 3 - Applied Loading after Decompression

The effect of increased moment after decompression on the stress distribution is shown in Figure 3(c). The final stresses in the bottom,  $f_{TtB}$  and top,  $f_{Tcx}$  of the glulam for the linear-elastic case are:

$$f_{TtB} = \sigma_{ta} = \varepsilon_{TtB} \cdot E_T \quad (13)$$

$$f_{Tcx} = \sigma_{cd} - \sigma_{ip} + \sigma_{ca} \quad (14)$$

where  $\sigma_{ta}$  = incremental tension stress due to applied moment,  $M$ .

$\sigma_{ca}$  = incremental compression stress due to applied moment,  $M$  (i.e.)  $\sigma_{ca} (y_{Ec, \max} / y_{Et, \max})$ .

The total tension stress in the FRP,  $\sigma_{Ft}$  at any time during stage 3 is determined by Equation 15:

$$\sigma_{Ft} = p_i + \sigma_{Fd} + \sigma_{Fa} \quad (15)$$

where  $p_i$  = initial pre-tension stress applied to the FRP (i.e.)  $P_i / A_F$ .

$\sigma_{Fd}$  = stress induced in the FRP due to the applied decompression moment,  $M_d$ .

$\sigma_{Fa}$  = stress induced in the FRP due to applied moments,  $M$  after decompression.

### 3. Results and Discussion

The features of the model were demonstrated using four different glulam configurations, modelled in four-point bending over a span of 3960mm. These consisted of 1 unreinforced control beam (C), 1 non-prestressed FRP reinforced glulam (R), and 2 prestressed FRP reinforced beams (P1, P2). The FRPs bonded to beams P1 and P2 were pre-tensioned to 25% and 50% of their UTS, respectively. The top glulam section was 195mm deep and 96mm wide. A 25mm deep bumper laminate and a 3.6mm thick FRP laminate of the same width were bonded to this top section to form a reinforced beam of total height,  $h_A$  equal to 223.6mm, as shown in Figure 2(a). The input values of timber ultimate tension,  $f_{Tu}$  and compression,  $f_{Tc}$  strength used in the models were 27.1 and 30.6 N/mm<sup>2</sup>, respectively, as reported by *Patrick (2004)* [8] for C16 grade Irish Sitka spruce. *Patrick (2004)* [8] also established that the slope of the plastic portion of the compressive  $\sigma - \varepsilon$  relationship is a ratio,  $m$  equal to 0.149 of the MOE of the timber. Machine grading was used to determine a mean MOE value of 7873 N/mm<sup>2</sup> for Irish Sitka spruce. The UTS and MOE of the FRP laminate applied in the model were 1000 N/mm<sup>2</sup> and 39000 N/mm<sup>2</sup>, respectively, as reported by *Patrick (2004)* [8] for a glass fibre/polyurethane resin FRP. Model predictions for stiffness, load-deflection and ultimate capacity at initial failure of the bumper laminate and global failure of the laminate above the FRP are summarised in Table 1.

Table 1 Analytical model stiffness and ultimate capacity results

Beam No. (#)	Beam Type (-)	Stiffness		Failure Mode (-)	Load - Deflection		Ultimate Capacity	
		Beam Lay - Up (-)	$E E I E$ (Nmm <sup>2</sup> x 10 <sup>12</sup> )		$W_{mu}$ (kN)	$\delta_c$ (mm)	$M_u$ (kNm)	$f_{mu}$ (N/mm <sup>2</sup> )
C	Unreinforced Control	With Bumper	0.674	(c) Bumper Laminate	39.80	68.3	26.27	34.15
		Without Bumper	0.482					
R	Non-Prestressed FRP $p_i = 0\%$ FRP UTS	With Bumper	0.777	(c) Bumper Laminate	55.62	96.1	36.71	44.75
		Without Bumper	0.589	(d) Laminate Above FRP	48.79	122.3	32.20	45.10
P2	Prestressed FRP $p_i = 50\%$ FRP UTS	With Bumper	0.777	(c) Bumper Laminate	78.99	94.6	52.13	44.98
		Without Bumper	0.589	(d) Laminate Above FRP	70.00	102.3	46.20	45.30
P1	Prestressed FRP $p_i = 25\%$ FRP UTS	With Bumper	0.777	(c) Bumper Laminate	96.86	102.5	63.93	46.30
		Without Bumper	0.589	(d) Laminate Above FRP	86.67	114.6	57.20	46.64

The FRP reinforced beams show an increase of 15% in stiffness with the addition of only 1.64% reinforcement. The upward pre-camber deflection also effectively increases the stiffness of the prestressed glulams. The moment capacity,  $M_u$  of the control beam, before the bumper laminate fails, is increased by 98% and 143% when reinforced with a FRP laminate prestressed to 25% and 50% of its UTS, respectively, in comparison with 40% when the same FRP is not pre-tensioned.

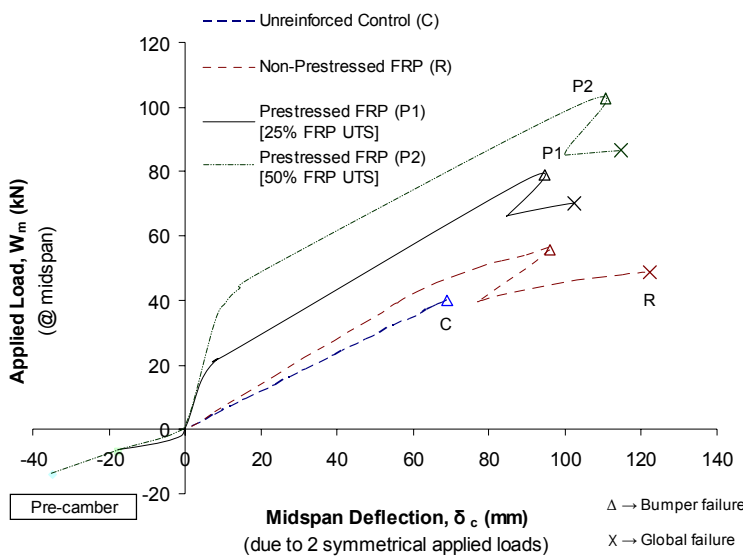


Fig. 4 Theoretical load,  $W_m$  versus deflection,  $\delta_c$

The tension stress in the bumper laminate at failure in bending,  $f_{mu}$  for beam P1 and P2 increases by 32% and 36%, respectively, in comparison with 31% for beam R. This increase due to the presence of the FRP is briefly discussed in Section 2.2.

The predicted midspan deflection,  $\delta_c$  due to two symmetrical applied loads,  $W_m/2$  for all the beams is illustrated in Figure 4. The behaviour of the unreinforced beam (C) is essentially linear, representing a near pure tension fracture. The relationship for the non-prestressed and prestressed FRP reinforced beams is similar and can be considered to consist of a number of distinct regions: the linear-elastic phase, the elastic-plastic phase before the bumper fails, bumper failure and the post bumper failure phase.

For the non-prestressed FRP reinforced case, after the initial linear-elastic phase, the effect of plastic yielding of the timber compression face, as the ultimate load,  $W_{mu}$  of the bumper is approached, is illustrated. The load carrying capacity then decreases rapidly when the bumper laminate fails. As the FRP laminate is assumed to remain undamaged, during the post bumper failure phase, the load capacity increases again until global failure of the glulam above the FRP occurs. For the prestressed beams, the negative pre-camber deflection, due to a constant hogging moment,  $M_p$ , is plotted. The early portion of the positive deflection response represents the decompression stage. The ultimate load of the prestressed beams, P1 and P2 is 98% and 143% greater than that of the unreinforced beam (C), whereas the non-prestressed beam (R) shows a 40% increase. In addition, beams R, P1 and P2 are more ductile than the control beam, deflecting 80%, 50% and 68%, respectively, more at failure of the laminate above the FRP. This indicates that prestressed beams have a higher load capacity but are less ductile than the non-prestressed FRP reinforced glulam.

#### 4. Conclusions

The analytical models presented in this paper suggest that the bonding of pre-tensioned FRP laminates in the tension zone of low-grade glulam beams can significantly improve their flexural strength and ductility. Eccentric prestressing also effectively increases the stiffness by introducing an upward pre-camber to offset deflection under loading. The models developed take into account the plastic behaviour of timber in compression and different failure modes of FRP reinforced beams, incorporating a bumper laminate, are considered.

In the next phase of the research, the models will be validated and calibrated with the results of full-scale tests. In addition, further research is necessary to investigate the effect of short-term elastic shortening and long-term creep of the timber on prestress loss.

#### 5. Acknowledgements

The authors gratefully acknowledge the financial support of the Irish Research Council for Science, Engineering and Technology (IRCSET).

#### 6. References

- [1] Martin Z.A., Stith J.K., & Tingley D.A. "Commercialisation of FRP reinforced glulam beam technology", *Proceedings of the 6<sup>th</sup> World Conference on Timber Engineering (WCTE)*, Whistler, University of British Columbia, Canada, 2000.
- [2] Peterson J.L., "Wood beams prestressed with bonded tension elements", *ASCE Journal of Structural Division*, Vol. 91, No. 1, 1965, pp. 103 - 119.
- [3] Triantafillou T.C. & Deskovic N., "Prestressed FRP sheets as external reinforcement of wood members", *ASCE Journal of Structural Engineering*, Vol. 118, No. 5, 1992, pp. 1270 - 1284.
- [4] Rodd P.D. & Pope D.J., "Prestressing as a means of better utilising low quality wood in glued laminated beams", *Proceedings of the International Conference on Forest Products*, Daejeon, Korea, 2003.
- [5] Romani M. & Blaß H.J., "Design model for FRP reinforced glulam beams", *Proceedings of the International Council for Research and Innovation in Building and Construction (CIB)*, Working Commission W18 - Timber Structures, Meeting 34, Venice, Italy, 2001.
- [6] Buchanan A.H. "Bending strength of lumber", *ASCE Journal of Structural Engineering*, Vol. 116, No. 5, 1990, pp. 1213 - 1229.
- [7] Piyong Yu., Silva P.F., & Nanni A. "Flexural strength of reinforced concrete beams strengthened with prestressed carbon fiber-reinforced polymer sheets – Part II", *ACI Structural Journal*, Vol. 105, No. 1, 2008, pp. 11 - 20.
- [8] Patrick G.R.H. "The structural performance of FRP reinforced glued laminated beams made of homegrown Sitka spruce", *Ph.D. Thesis*, 2004, Queen's University, Belfast, Northern Ireland.